ORIGINAL RESEARCH

Diffusion Tensor Imaging of the Optic Nerve in Subacute Anterior Ischemic Optic Neuropathy at 3T

M.-Y. Wang
P.-H. Qi
D.-P. Shi

BACKGROUND AND PURPOSE: DTI can provide in vivo information about the pathology of optic nerve disease, but there is no study of DTI in the setting of ION, the most frequent acute optic neuropathies in patients over 50 years of age. Our aim was to investigate the potential of DTI in the diagnosis of subacute AION at 3T.

MATERIALS AND METHODS: Twenty-six patients with unilateral AION and 15 healthy controls were enrolled in this study. DTI and pattern VEP were performed on the ONs of all subjects. The mean ADC, FA, and eigenvalue maps were obtained for quantitative analysis. Quantitative electrophysiology was also performed on all subjects.

RESULTS: The mean ADC and orthogonal eigenvalue $\lambda_\perp$ in affected nerves increased, and the mean FA was reduced compared with clinically unaffected contralateral nerves ($P < .001$) and control nerves ($P < .001$). However, no significant changes of the mean principal eigenvalue $\lambda_\parallel$ in affected nerves compared with unaffected contralateral nerves ($P = .13$) and control nerves ($P = .14$) were seen. There was a significant correlation of whole-field VEP amplitude with ADC ($r = -0.63$, $P = .001$) and $\lambda_\perp$ ($r = -0.47$, $P = .015$) but no correlation with FA ($P = .06$) and $\lambda_\parallel$ ($P = .06$).

CONCLUSIONS: DTI measurement of ischemic ONs provides in vivo information about pathology and may serve as a biomarker of axonal and myelin damage in AION.

ABBREVIATIONS: AAION = arteritic anterior ischemic optic neuropathy; ADC = apparent diffusion coefficient; AION = anterior ischemic optic neuropathy; DTI = diffusion tensor imaging; EPI = echo-planar imaging; FA = fractional anisotropy; GRAPPA = generalized autocalibrating partially parallel acquisition; ION = ischemic optic neuropathy; IPAT = integrated parallel acquisition technique; $\lambda_\perp$ = orthogonal eigenvalue; $\lambda_\parallel$ = principal eigenvalue; MD = mean diffusivity; ON = optic nerve; PION = posterior ischemic optic neuropathy; SE = spin-echo; VEP = visual-evoked potentials; ZOOM = zonal oblique multisection

ION is one of the most prevalent and visually crippling diseases in the middle-aged and elderly population. Generally it is caused by interruption of blood flow in the ophthalmic artery or its branches, resulting in varying degrees of blindness. ION is classified into AION and PION, according to the affected part of the ON.[1] The AION involves the ON head supplied by the posterior ciliary artery, while the PION is not secondary to an ischemic disorder of any particular artery. Optic disc edema from ischemia to the anterior nerve is present in AION and absent in PION. AION is the most common and is further categorized as either AAION, caused by vasculitis involving the short posterior ciliary arteries, or nonarteritic AION, caused by hypoperfusion (mechanism unknown) within the microcirculation of the optic disc. AAION, classically due to temporal arteritis, is an ophthalmologic emergency, requiring prompt recognition and treatment to prevent devastating blindness. The diagnosis of AION is primarily based on clinical findings combined with the visual field and laboratory tests. Because the diameter of the optic nerve is only approximately 3–7 mm and the vessels that supply blood to it are very thin, it is challenging to detect the ION by imaging.

Conventional MR imaging provides little information regarding AION, limited to orbital fat enhancement and ON and nerve sheath enhancement from vasculitis,[2] and it fails to accurately assess the underlying pathophysiology preceding the irreversible structural damage. DTI is a widely recognized imaging technique used to study the connectivity and integrity of white matter in the central nervous system tissues.[3-5] The usefulness of diffusion imaging in cerebral ischemia is that it not only predicts the presence of significant ischemia within minutes of the onset of injury but also demonstrates subacute and chronic ischemia. Because the ON is actually a conduction tract of the central nervous system,[6,7] the pathophysiology of ON ischemia is expected to be similar to that seen in the brain, specifically cell swelling and abnormality of water diffusion leading to changes of ADC and FA.

Some previous studies in which DTI was performed on the ON in patients with optic neuritis revealed changes of DTI measurement and its association with the electrophysiologic or clinical parameters.[8,9] However, to our knowledge, there is no study of the application of DTI in the setting of ION because of the technical challenges. In this study, we aimed to investigate the value of quantitative DTI in assessing the axonal and myelin damage in AION by

Received October 1, 2010; accepted after revision November 26.

From the Department of Radiology, Henan Provincial People's Hospital, Zhengzhou, Henan, China.

Please address correspondence to Da-Peng Shi, MD, Department of Radiology, Henan Provincial People's Hospital, 7 Weiwu Rd, Zhengzhou, Henan 450003, China.; e-mail: cjr.shidapeng@vip.163.com

DOI 10.3174/ajnr.A2487

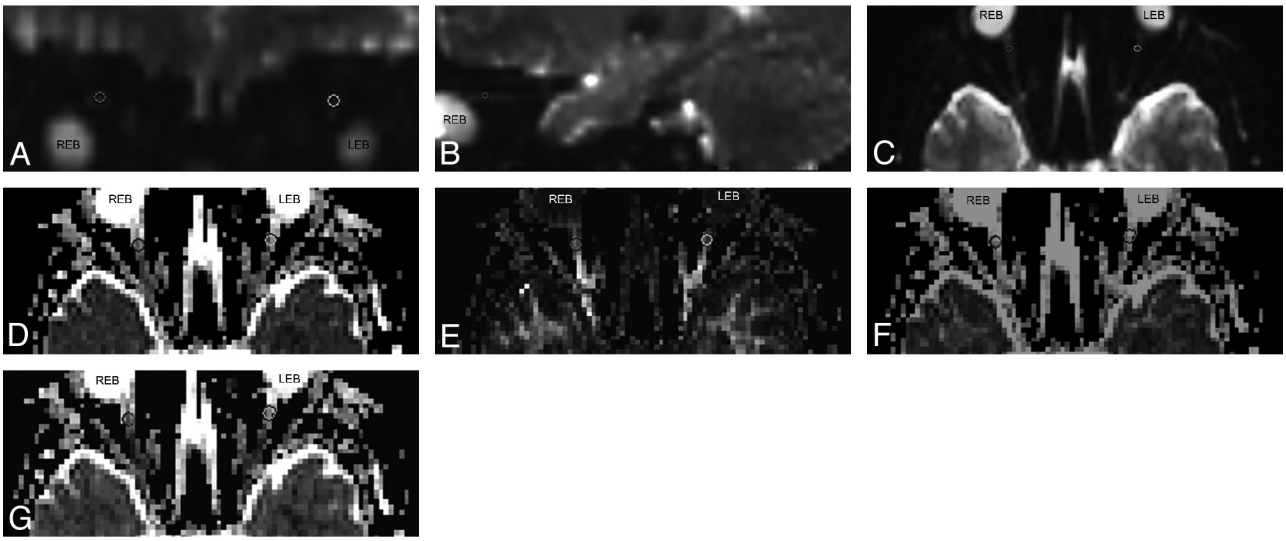

Fig 1. *A–C*, DTI maps of the central section of the ON. The regions of interest are placed on the b=0 averaged images, which are defined in the coronal map (*A*) and adjusted in the sagittal (*B*) and axial (*C*) images obtained by using multiplanar reconstruction. *D–G*, Then the regions of interest are transferred onto the ADC (*D*), FA (*E*), $\lambda_{\|}$ (*F*), and $\lambda_{\perp}$ (*G*) maps.

using high-field MR imaging (3T). We hypothesized that quantitative DTI may be useful in assessing the axonal and myelin damage in AION and that changes may be related to measures of electrophysiologic markers of ON function. Thus in this study, we compared the DTI results in 26 patients with AION in the subacute period following injury with those obtained in healthy controls and correlated these with quantitative electrophysiology.

Materials and Methods

Subjects

Twenty-six patients (14 men, 12 women; mean age, 52 years; range, 28–70 years) with unilateral AION were retrospectively recruited for this study from July 2008 to October 2009. No patient had a history of trauma, optic neuritis, or abnormal electroretinogram findings. Each patient underwent a complete ophthalmologic examination. Diagnosis of AION was made according to the following criteria: 1) a history of sudden or rapidly progressive visual loss secondary to an optic neuropathy; 2) documentation of optic disc edema at the time of visual loss; 3) no evidence of another neurologic or ocular disorder that may be responsible for optic disc edema and visual impairment; and 4) specific exclusion of other causes of optic neuropathy, especially inflammatory optic neuritis, by lack of pain on eye movement, lack of substantial improvement on follow-up, and lack of optic nerve enhancement on neuroimaging.[10]

Fifteen healthy volunteers were enrolled in this study. None had any ophthalmologic or neurologic disorders. The mean age was 50 years (range, 30–58 years) with 8 women and 7 men. One eye from each control subject was randomly chosen for study.

This study was approved by the local ethics committees, and all subjects provided informed consent in writing in accordance with the Declaration of Helsinki.

MR Imaging Acquisition

Subjects were instructed to focus their vision on a fixation point during MR imaging to reduce motion artifacts. Routine MR imaging of the brain was performed to exclude intracranial diseases on a 3T scanner (Magnetom Trio; Siemens, Erlangen, Germany) with a maximum gradient strength of 40 mT/m and a 12-channel head coil. The high-resolution anatomic 3D T1-weighted images were acquired by using a magnetization-prepared rapid acquisition of gradient echo sequence with an isotropic voxel resolution of 1 mm. DTI of the ONs was obtained by using an SE-EPI sequence with the following parameters: TR, 5000 ms; TE, 97 ms; FOV, 230 × 230 mm; matrix size, 256 × 256; b = 1000 s/mm^2; section thickness, 2 mm; and 64 diffusion-gradient directions. Parallel imaging by using GRAPPA with an IPAT factor of 2 was applied. Approximately 60 axial sections with zero intersection gap were acquired to cover the whole brain. The acquisition time was 5 minutes 42 seconds.

The postprocessing of DTI was performed by using NEURO 3D on the syngo MR B15 workstation (Siemens). ADC, FA, and eigenvector maps were calculated on a pixel-by-pixel basis. Each ON was manually segmented by a neuroradiologist blinded to the clinical status of the patient, from the $b = 0$ image on the section on which the intraorbital nerve was clearly seen. The region of interest including the ON was manually placed over the anterior segment of each ON on the non-diffusion weighted (b_0) image, which was defined in the coronal map and adjusted in the axial and sagittal images obtained by using multiplanar reconstruction (Fig 1). The regions of interest were then transferred to the corrected ADC, FA, and eigenvector maps (Fig 1). The mean ADC, FA, principal eigenvalue ($\lambda_{\|}$), and the average of the 2 orthogonal eigenvalues ($\lambda_{\perp}$) of the affected ON, unaffected nerve of each patient, and 1 of the ONs of each control subject were obtained respectively.

VEP Examination

The electrophysiologic examination of ONs was performed in a dark room on a Keypoint evoked-potential monitor (Dantec, Copenhagen, Denmark). Subjects were instructed to focus their vision on the red dot in the middle of the screen with their eyes 100 cm away from the screen. The active electrode, reference electrode, and ground electrode were put about 2 cm above occipital tuberosity, in the middle of forehead, and on the ear lobes, respectively. The stimulus form was a black and white inversion checkerboard square with the following parameters: inversion frequency, 2 Hz; contrast, 80%; average brightness, 50 candela/m^2; analyze time, 250 ms; fold, 200.

Table 1: Demographic data and visual function of patients[a]

	Mean	SD	Range	Ratio
Male/female	–	–	–	14:12
Age (yr)	53.23	9.53	27–69	–
Time[b]	20.65	8.84	6–30	–
Standard logarithmic visual acuity				
Affected	0.22	0.21	0.01–0.80	–
Not affected	0.97	0.16	0.6–1.2	–
Visual field mean deviation (dB)				
Affected	22.98	5.95	10.93–32	–
Not affected	1.72	1.87	0.10–7.70	–

[a] —indicates patients with AION.
[b] Since onset of AION (days).

Table 2: Demographic data and visual function of controls

	Mean	SD	Range	Ratio
Male/female				8:7
Age (yr)	50	8.23	30–58	
Standard logarithmic visual acuity, selected	1.12	0.11	0.8–1.4	
Visual field mean deviation (dB), selected	1.56	1.22	0.1–6.2	

Statistical Analysis

Statistical analyses were performed by using the Statistical Package for the Social Sciences, Version 11.5 for Windows (SPSS, Chicago, Illinois). Differences between the affected eye and unaffected eye within patients were explored by using the Wilcoxon signed rank test, and differences between patients and controls were evaluated by using the Wilcoxon rank sum test. Spearman rank correlations were calculated among MR imaging parameters, electrophysiologic variables, and visual function as well.

Results

Clinical Data of Patients

Tables 1 and 2 summarize characterizations and demographics of patients and controls, including the range of visual function.

Associated Risk Factors

In 26 patients, 9 (35%) had arterial hypertension, 5 (19%) had diabetes mellitus, and 3 (12%) had both arterial hypertension and diabetes mellitus. Seven of 26 patients (27%) had hypercholesterolemia by history or laboratory testing, and 2 patients (8%) had obesity. Eight patients (31%) smoked cigarettes, 3 (12%) had ischemic heart disease, and 1 (4%) had a previous stroke.

Routine MR Imaging

There was no abnormality in the shape and signal intensity of the ON in 26 patients with unilateral AION on routine brain MR imaging.

Group Differences in DTI Parameters and Electrophysiologic Data

Table 3 presents the DTI parameters and electrophysiologic data.

The mean whole-field VEP amplitude from affected nerves was lower at 4.53 ± 1.17 μV, compared with clinically unaffected contralateral nerves at 9.67 ± 2.52 μV ($P < .001$ versus affected nerves) and 9.40 ± 3.03 μV from control nerves ($P < .001$ versus affected nerves). There was no significant difference between control nerves and unaffected contralateral nerves of patients ($P = .44$).

The mean whole-field VEP latency from affected nerves was higher at 132.7 ± 17.48 ms, compared with 94.86 ± 9.07 ms from clinically unaffected contralateral nerves ($P < .001$ versus affected nerves) and 97.77 ± 4.62 ms from control nerves ($P < .001$ versus affected nerves). There was no significant difference between nerves of controls and unaffected contralateral nerves of patients ($P = .06$).

The mean ADC from affected nerves was higher at 1429 ± 198 × 10^{-6} mm^2s^{-1}, compared with 1028 ± 146 × 10^{-6} mm^2s^{-1} from clinically unaffected contralateral nerves ($P < .001$ versus affected nerves) and 1008 ± 111 × 10^{-6} mm^2s^{-1} from control nerves ($P < .001$ versus affected nerves). There was no significant difference between nerves of controls and unaffected contralateral nerves of patients ($P = .89$).

The mean FA from affected nerves was lower at 0.283 ± 0.073, compared with 0.569 ± 0.046 from clinically unaffected contralateral nerves ($P < .001$) and 0.587 ± 0.023 from nerves of controls ($P < .001$). There was no significant difference between nerves of controls and unaffected contralateral nerves of patients ($P = .09$).

The mean principal eigenvalue $\lambda_{\parallel}$ in affected nerves was 1786 ± 159 × 10^{-6} mm^2s^{-1} compared with 1720 ± 199 × 10^{-6} mm^2s^{-1} in unaffected contralateral nerves ($P = .14$) and 1702 ± 199 × 10^{-6} mm^2s^{-1} in control nerves ($P = .13$). There was no significant difference between nerves of controls and unaffected contralateral nerves of patients ($P = .73$).

The mean orthogonal eigenvalue $\lambda_{\perp}$ from affected nerves was elevated at 1245 ± 172 × 10^{-6} mm^2s^{-1}, compared with 746 ± 78 × 10^{-6} mm^2s^{-1} from clinically unaffected contralateral nerves ($P < .001$) and 729 ± 130 × 10^{-6} mm^2s^{-1} from nerves of controls ($P < .001$). There was no significant difference between nerves of controls and unaffected contralateral nerves of patients ($P = .79$).

Figure 2 compares the DTI measures of the affected ON of patients with the unaffected contralateral ON and normal ON of controls.

Correlation of DTI Data with Electrophysiology and Visual Function

There was a significant correlation of the whole-field VEP amplitude with ADC ($r = -0.63$, $P = .001$) and $\lambda_{\perp}$ ($r = -0.47$, $P = .015$) in affected eyes (Fig 3); there were no significant trends for correlation of affected eye FA and $\lambda_{\parallel}$ with whole-field VEP amplitude. No correlation was found with any of the DTI measures and clinical measures of visual function, including visual acuity and visual field ($P > .05$).

Discussion

The ON is a simple and well-defined white matter tract emanating from retinal ganglion cells. Although conventional MR imaging has been used to detect ON atrophy and sheath dilation,[11,12] performing in vivo diffusion measurements on the human ON remains very challenging because of its small size, motion, the presence of magnetic field susceptibility artifacts,

Table 3: DTI parameter and electrophysiologic group data[a]

	FA[b,c]	ADC ($\times 10^{-6}$ mm^2s^{-1})[b,c]	$\lambda_{\|}$ ($\times 10^{-6}$ mm^2s^{-1})	$\lambda_{\perp}$ ($\times 10^{-6}$ mm^2s^{-1})[b,c]	Whole-Field VEP Amplitude (μV)[b,c]	Whole-Field VEP Latency (ms)[b,c]
Patients' affected nerves ($n = 26$)	0.283 ± 0.073	1429 ± 198	1786 ± 159	1245 ± 172	4.53 ± 1.17	132.7 ± 17.48
Patients' unaffected nerves ($n = 26$)	0.569 ± 0.046	1028 ± 146	1720 ± 199	746 ± 78	9.67 ± 2.52	94.86 ± 9.07
Control nerves ($n = 15$)	0.587 ± 0.023	1008 ± 111	1702 ± 199	729 ± 130	9.40 ± 3.03	97.77 ± 4.62

[a] The values are mean ± SD.
[b] Significant difference between nerves of controls and affected nerves of patients.
[c] Significant difference between unaffected contralateral nerves and affected nerves in patients. There is no significant difference between unaffected ONs of patients and ONs of controls in all DTI measures.

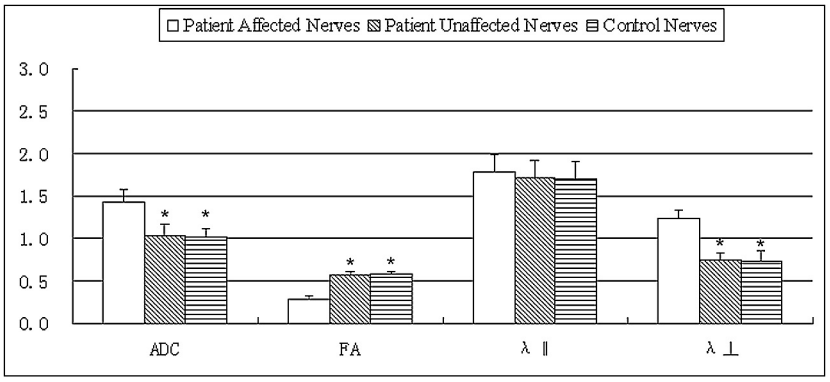

Fig 2. Bar graphs of the ADC, FA, principal eigenvalue $\lambda_{\|}$, and the orthogonal eigenvalues $\lambda_{\perp}$ averaged across the affected and unaffected contralateral ONs of 26 patients with ION compared with normal ONs of 15 controls. The error bars denote the SDs across subjects. The units of the ADC, $\lambda_{\|}$, and $\lambda_{\perp}$ measures are in $\times 10^{-3}$ square millimeters per second $^{-1}$. The asterisk indicates a significant difference compared with the affected nerves of patients. There is no significant difference between unaffected ONs of patients and ONs of controls in all DTI measures.

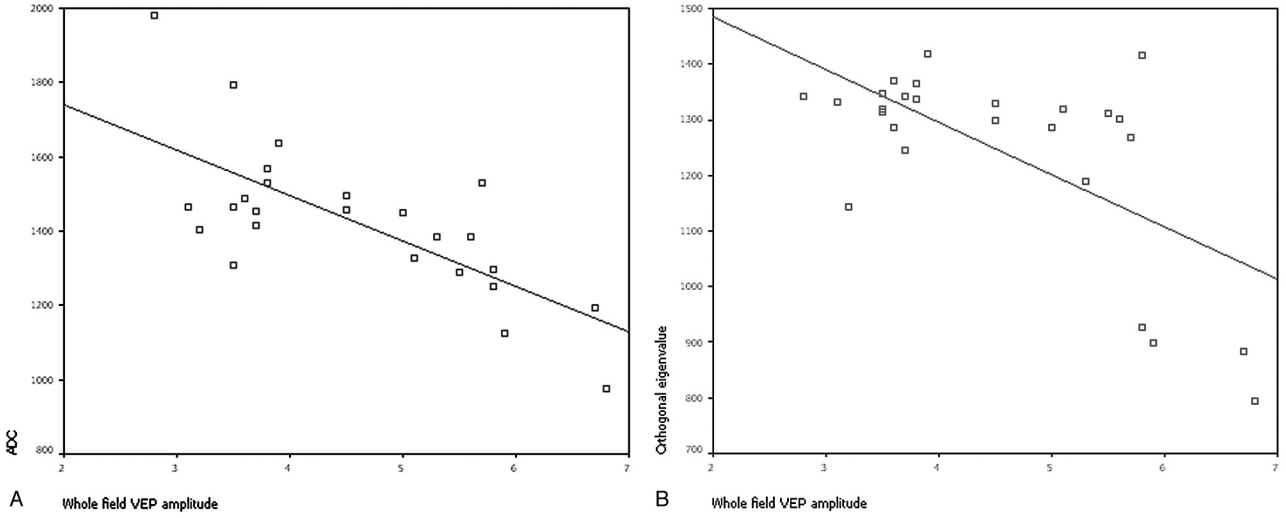

Fig 3. Plot of ADC (*A*) and the orthogonal eigenvalue $\lambda_{\perp}$ (*B*) versus whole-field VEP amplitude averaged across the pixels inside the regions of interest along the affected ONs of 26 patients with ischemic ION, respectively.

and high signal intensity from the surrounding orbital fat and CSF.

In DTI, ADC is a widely used parameter that measures the magnitude of diffusion of water molecules within cerebral tissue. FA measures the fraction of the magnitude of diffusivity that can be ascribed to anisotropic diffusion, which is thought to reflect fiber attenuation, axonal diameter, and myelination in white matter. FA is calculated from the 3 eigenvalues (λ_1, λ_2, λ_3) of the diffusion tensor. Of the 3 eigenvalues, the largest is the principal eigenvalue ($\lambda_{\|}$), representing the diffusion coefficient along the principal direction of diffusion parallel to the nerve; the other 2 are the diffusion coefficients orthogonal to the nerve. The average of the 2 orthogonal eigenvalues is expressed as $\lambda_{\perp}$.

Hickman et al[8] used ZOOM EPI to determine in vivo ADC changes in patients with optic neuritis. Their results showed that the mean ADC of the affected ON correlated with the clinical and electrophysiologic parameters in the chronic ON lesions; their findings suggest that the ADC value is a potential surrogate measure of axonal disruption in the chronic postinflammatory ON lesion. However, DTI parameters, such as FA, are sensitive to the underlying structure of the tissue and are expected to be particularly sensitive to pathologic changes such as edema and myelin

loss. Diffusion measurements in animal models and excised tissues have shown the importance of measuring anisotropy, as well as contributions from $\lambda_{\parallel}$ and $\lambda_{\perp}$, to various pathologies such as axonal and myelin injury.[13-16]

A study[9] of patients with optic neuritis by using the ZOOM DTI technique revealed abnormalities within the ON, consisting of elevation of the mean orthogonal eigenvalue $\lambda_{\perp}$ and MD and reduction of the mean FA in affected nerves compared with clinically unaffected contralateral nerves and control nerves. The mean principal eigenvalue $\lambda_{\parallel}$ was significantly increased in affected nerves compared with contralateral unaffected nerves but not compared with control nerves. There was a significant correlation of the whole-field VEP amplitude with MD ($r = -0.57$, $P = .006$) and $\lambda_{\perp}$ ($r = -0.56$, $P = .007$). Their results suggest that ON DTI measurements may provide an indication of the structural integrity of axons. Wheeler-Kingshott et al[17] also used a ZOOM DTI technique in healthy controls and derived the mean FA, $\lambda_{\parallel}$, and $\lambda_{\perp}$ values of the ONs on both sides across 10 healthy volunteers.

The ZOOM technique is not the only one able to evaluate the ON with full diffusion tensor measurements. For example, Koch et al[18] performed DTI by using a single-shot stimulated-echo acquisition mode with center-out phase-encoding, which has the advantage of being less sensitive to susceptibility-induced artifacts, and generated images of the ON on DTI parameter maps such as FA. Chabert et al[19] used another type of acquisition method (non-Care-Purcell-Meiboom-Gill fast spin-echo) and obtained results very similar to those of Wheeler-Kingshott.[17]

A conventional DTI protocol was modified by Techavipoo et al[20] to acquire images with fat and CSF suppression and field inhomogeneity maps of contiguous coronal sections covering the whole brain. The technique was applied to healthy volunteers and patients with multiple sclerosis with and without a history of unilateral optic neuritis. They found that ON tractography became feasible after distortion correction. The diffusion measurements from the healthy volunteers were in good agreement with the literature. The diffusion measurements before and after geometric distortion correction were not significantly different. Thus a practical DTI protocol was provided to study the human ON.

In our study, a high-field MR imaging scanner (3T) and increased gradient strength (40 mT/m) with a 12-channel head coil were used to improve the signal intensity–to-noise ratio, an SE-EPI DTI sequence with a higher resolution ($0.90 \times 0.90 \times 2\ mm^3$) was applied to decrease partial volume, and 64 directions were used to obtain better diffusion maps of the ONs. The signal intensity from surrounding fat was suppressed by using a selective spectral-spatial pulse (exciting only water) for excitation, to reduce the partial volume effects. Twice-refocused SE together with a bipolar gradient in the EPI sequence was used to reduce eddy currents. Parallel imaging (GRAPPA, IPAT factor = 2) was used to accelerate the image acquisition and reduce distortion. In this method, the mean FA, $\lambda_{\parallel}$, and $\lambda_{\perp}$ across 15 healthy volunteers were $0.587 \pm 0.023 \times 10^{-6}\ mm^2s^{-1}$, $1702 \pm 199 \times 10^{-6}\ mm^2s^{-1}$, and $729 \pm 130 \times 10^{-6}\ mm^2s^{-1}$, respectively, which were comparable with the results of Techavipoo et al[20] (0.48 ± 0.030, $1651 \pm 219 \times 10^{-6}\ mm^2s^{-1}$, and $815 \pm 113 \times 10^{-6}\ mm^2s^{-1}$, respectively) from the control ONs on the left side. The mean ADC from control nerves was $1008 \pm 111 \times 10^{-6}\ mm^2s^{-1}$, which was similar to that of Hickman et al ($928 \pm 23 \times 10^{-6}\ mm^2s^{-1}$).[8]

The ADC value represents the diffusivity of water molecules. In cerebral ischemia, restriction in water diffusion occurs within minutes of the onset of ischemic injury. The ADC reaches the lowest value within 24 hours and then slowly increases to reach normal values in approximately 7–10 days.[21] It then increases and remains at supernormal values. This process is explained by the conversion of cytotoxic edema to vasogenic edema and the increased water content of the tissue. Theoretically, the changes of ADC in ION should be similar to those in cerebral ischemia. Al-Shafai and Mikulis[22] reported the findings of diffusion-weighted imaging in a patient with acute ION, and their results demonstrated that the ADC value was decreased at day 2 after the patient's acute worsening. However, our study found that ADC increased significantly and FA reduced significantly in affected ONs compared with unaffected contralateral nerves and nerves of healthy controls, because in our study, the time course between onset and imaging of all patients was from 6 to 30 days, during which the ADCs should be normal or increased rather than decreased. These results are in keeping with the expected ADC pattern as seen in ischemic injury to the brain in the same stage. The ADCs may decrease in acute ION as Al-Shafai and Mikulis reported.[22]

Future studies on acute ION would be helpful to obtain the temporal evolution of ADCs in ION. The VEP amplitude is believed to reflect the number of ON fibers in functional continuity.[23] The significant correlation of VEP amplitude reduction with ADC increase in the clinically affected eyes suggests that the increased diffusivity is of functional relevance and may reflect axonal disruption or loss and demyelination.

FA is the most widely used measure of anisotropy in DTI. In this study, the mean FA from affected nerves was lower than that from clinically unaffected contralateral nerves and control nerves; this finding most probably reflects vasogenic edema and the increased water content of tissue, cell lysis, and axonal loss of ONs. However, FA does not describe the full tensor shape or distribution because different eigenvalue combinations can generate the same FA values.[24] Thus eigenvalues may be more sensitive than FA in quantifying pathology. This difference may explain the finding that the mean FA decreased significantly in affected nerves but did not correlate with whole-field VEP amplitude in this study. Several recent studies have also suggested that the eigenvalue amplitudes or combinations of the eigenvalues (eg, $\lambda_{\perp}$) demonstrate more specific relationships to white matter pathology.[25] The mean of the orthogonal eigenvalues, $\lambda_{\perp}$, reflects diffusion orthogonal to the axis of the ON, whereas $\lambda_{\parallel}$ represents the diffusion coefficient along the principal direction of diffusion parallel to the nerve. In this study, $\lambda_{\perp}$ changed similar to ADC in that it was significantly increased in affected nerves and correlated with whole-field VEP amplitude. However, the principal eigenvalue, $\lambda_{\parallel}$, was not significantly different among the 3 groups of ONs. These results were similar to those in optic neuritis,[16] and the possible mechanism for

this may be that though some axons are lost following optic ischemia, the remaining axons are still aligned in the same direction along the ON, so the $\lambda_{\parallel}$ is relatively normal.

The current study did not find an association of any DTI parameter with measures of visual function. A previous study by Hickman et al[11] used ZOOM EPI to study the optic nerve in 16 patients with optic neuritis at the same 1-year period and found that the ADC of the affected nerve correlated with measures of visual function. However, another study of patients with optic neuritis by Trip et al[9] by using the ZOOM DTI technique did not find an association of any DTI parameters with measures of visual function, which was consistent with the results of this study. This finding may be explained by the fact that the disease duration in the present study was heterogeneous and DTI measures of ION have different recovery processes compared with optic neuritis. Larger samples of patients with ION with the same disease duration may be helpful in revealing the association of DTI measures with clinical severity, treatment effect, and prognosis. Although there was no correlation between any DTI measures and visual function in the present study, DTI detected the changes of ADC, FA, and $\lambda_{\perp}$ in affected eyes when routine MR imaging findings were normal. Thus DTI measures should be helpful in the diagnosis of ION.

AION typically occurs after 55 years of age, but it can also occur in younger patients. The most important risk factors for developing AION include hypertension, nocturnal hypotension, diabetes mellitus, atherosclerosis, and a small cup in the optic disc. Our results were consistent with the reports.[26] In patients younger than 50 years, diabetes mellitus, hypertension, and hypercholesterolemia are associated more strongly with AION than in older individuals.[27,28] In our study, 6 of 26 patients were younger than 50 years. In these 6 patents, 2 had arterial hypertension, 1 had diabetes mellitus, 1 had both arterial hypertension and diabetes mellitus, and 2 had hypercholesterolemia. Therefore, AION should be considered in the differential diagnosis of younger patients with painless optic neuropathy with disc edema at presentation, and these patients require a thorough systemic evaluation for underlying vascular risk factors.

Several limitations of the current study should be addressed. First, to develop a practical protocol with a shorter acquisition time, our approach does not use the CSF suppression technique in DTI of the ON. Because the ON is surrounded by CSF, suppression of CSF signals would purify signals of the ON. Some previous studies have shown that signals from CSF cause underestimation of the diffusion anisotropy measures such as FA.[29] However, our measurements of FA, $\lambda_{\parallel}$, and $\lambda_{\perp}$ were not lower than those in other reports.[20] This may be ascribed to a higher b-value ($b = 1000$ s/mm^2) and resolution ($0.90 \times 0.90 \times 2$ mm^3) with fat suppression to increase the accuracy of measurement, twice-refocused SE with a bipolar gradient in the EPI sequence to reduce eddy currents, and parallel imaging (GRAPPA, IPAT factor = 2) to accelerate the image acquisition and reduce distortion. Second, cardiac gating was not implemented in the current protocol, so the protocol may contain errors from different cardiac cycles. This problem may be alleviated by using high directional resolution of diffusion-weighted directions. However, it seemed that cardiac gating was not necessary for this study because the diffusion-weighted imaging and resultant maps (ADC, FA, and eigenvalues) were of good quality.

In addition, some reports showed that FA values of the brain white matter declined significantly with age in all regions except the splenium.[29,30] The FA values of the ON may also have similar changes with age in brain white matter. These changes would be expected to have some effect on the measurements. However, because we enrolled age- and sex-matched controls, this factor should have a similar effect on both groups and would be unlikely to affect the overall result. Because our protocol has a reasonable acquisition time, which was only 5 minutes 42 seconds, and the entire brain was scanned at the same time, it should be a practical one for the DTI study of the human ON and other parts of the brain without additional scans.

Conclusions

The present study has shown that DTI indices of the ON such as ADC and the orthogonal eigenvalue $\lambda_{\perp}$ can be obtained in vivo and provide information about axonal and myelin damage in AION, which is very helpful for the diagnosis of ION. The DTI of the ON may be a useful tool for studying the effect of novel therapies and to evaluate the prognosis in ION.

References

1. Hayreh SS. **Ischaemic optic neuropathy.** *Indian J Opthamol* 2000;48:171–94
2. Morganstern KE, Ellis BD, Schochet SS, et al. **Bilateral optic nerve sheath enhancement from giant cell arteritis.** *J Rheumatol* 2003;30:625–27
3. Le Bihan D, Mangin JF, Poupon C, et al. **Diffusion tensor imaging: concepts and applications.** *J Magn Reson Imaging* 2001;13:534–46
4. Huppi PS, Dubois J. **Diffusion tensor imaging of brain development.** *Semin Fetal Neonatal Med* 2006;11:489–97
5. Mori S, Zhang J. **Principles of diffusion tensor imaging and its applications to basic neuroscience research.** *Neuron* 2006;51:527–39
6. Rizzo JF 3rd, Andreoli CM, Rabinov JD. **Use of magnetic resonance imaging to differentiate optic neuritis and non-anterior ischemic optic neuropathy.** *Ophthalmology* 2002;109:1679–84
7. Hayreh SS. **Posterior ischemic optic neuropathy: clinical features, pathogenesis and management.** *Eye (Lond)* 2004;18:1188–206
8. Hickman SJ, Wheeler-Kingshott CA, Jones SJ, et al. **Optic nerve diffusion measurement from diffusion-weighted imaging in optic neuritis.** *AJNR Am J Neuroradiol* 2005;26:951–56
9. Trip SA, Wheeler-Kingshott C, Jones SJ, et al. **Optic nerve diffusion tensor imaging in optic neuritis.** *Neuroimage* 2006;30:498–505
10. Preechawat P, Bruce BB, Newman NJ, et al. **Anterior ischemic optic neuropathy in patients younger than 50 years.** *Am J Ophthalmol* 2007;144:953–60
11. Hickman SJ, Brierley CM, Brex PA, et al. **Continuing optic nerve atrophy following optic neuritis: a serial MRI study.** *Mult Scler* 2002;8:339–42
12. Hickman SJ, Miszkiel KA, Plant GT, et al. **The optic nerve sheath on MRI in acute optic neuritis.** *Neuroradiology* 2005;47:51–55
13. Beaulieu C. **The basis of anisotropic water diffusion in the nervous system: a technical review.** *NMR Biomed* 2002;15:435–55
14. Xu J, Sun SW, Naismith RT, et al. **Assessing optic nerve pathology with diffusion MRI: from mouse to human.** *NMR Biomed* 2008;21:928–40
15. Song SK, Sun SW, Ju WK, et al. **Diffusion tensor imaging detects and differentiates axon and myelin degeneration in mouse optic nerve after retinal ischemia.** *Neuroimage* 2003;20:1714–22
16. Sun SW, Liang HF, Le TQ, et al. **Differential sensitivity of in vivo and ex vivo diffusion tensor imaging to evolving optic nerve injury in mice with retinal ischemia.** *Neuroimage* 2006;32:1195–204
17. Wheeler-Kingshott CA, Trip SA, Symms MR, et al. **In vivo diffusion tensor imaging of the human optic nerve: pilot study in normal controls.** *Magn Reson Med* 2006;56:446–51
18. Koch MA, Glauche V, Finsterbusch J, et al. **Distortion-free diffusion tensor imaging of cranial nerves and of inferior temporal and orbitofrontal white matter.** *Neuroimage* 2002;17:497–506
19. Chabert S, Molko N, Cointepas Y, et al. **Diffusion tensor imaging of the human optic nerve using a non-CPMG fast spin echo sequence.** *J Magn Reson Imaging* 2005;22:307–10
20. Techavipoo U, Okai AF, Lackey, et al. **Toward a practical protocol for human**

optic nerve DTI with EPI geometric distortion correction. *J Magn Reson Imaging* 2009;30:699–707
21. Yamada I, Kuroiwa T, Endo S, et al. **Temporal evolution of apparent diffusion coefficient and T2 value following transient focal cerebral ischemia in gerbils.** *Acta Neurochir Suppl* 2003;86:147–51
22. Al-Shafai LS, Mikulis DJ. **Diffusion MR imaging in a case of acute ischemic optic neuropathy.** *AJNR Am J Neuroradiol* 2006;27:255–57
23. Jones SJ, Brusa A. **Neurophysiological evidence for long-term repair of MS lesions: implications for axon protection.** *J Neurol Sci* 2003;206:193–98
24. Alexander AL, Hasan K, Kindlmann G, et al. **A geometric comparison of diffusion anisotropy measures.** *Magn Reson Med* 2000;44:283–91
25. Song SK, Sun SW, Ramsbottom MJ, et al. **Dysmyelination revealed through MRI as increased radial (but unchanged axial) diffusion of water.** *Neuroimage* 2002;17:1429–36
26. Rucker JC, Biousse V, Newman NJ. **Ischemic optic neuropathies.** *Curr Opin Neurol* 2004;17:27–35
27. Hayreh SS, Joos KM, Podhajsky PA, et al. **Systemic diseases associated with nonarteritic anterior ischemic optic neuropathy.** *Am J Ophthalmol* 1994;118:766–80
28. Deramo VA, Sergott RC, Augsburger JJ, et al. **Ischemic optic neuropathy as the first manifestation of elevated cholesterol levels in young patients.** *Ophthalmology* 2003;110:1041–45
29. Bhagat YA, Beaulieu C. **Diffusion anisotropy in subcortical white matter and cortical gray matter: changes with aging and the role of CSF-suppression.** *J Magn Reson Imaging* 2004;20:216–27
30. Pfefferbaum A, Sullivan EV, Hedehus M, et al. **Age-related decline in brain white matter anisotropy measured with spatially corrected echo-planar diffusion tensor imaging.** *Magn Reson Med* 2000;44:259–68